Design and Development of High Efficiency Five Stage Battery Charge Controller With Improved MPPT Performance for Solar PV Systems

Joydip Jana*‡, Hiranmay Samanta**, Konika Das Bhattacharya***, Hiranmay Saha****

*Centre of Excellence for Green Energy and Sensor Systems, IIEST, Shibpur, Howrah, West Bengal, India

**Centre of Excellence for Green Energy and Sensor Systems, IIEST, Shibpur, Howrah, West Bengal, India

***Department of Electrical Engineering, IIEST, Shibpur, Howrah, West Bengal, India

****Centre of Excellence for Green Energy and Sensor Systems, IIEST, Shibpur, Howrah, West Bengal, India

(joydipjana02@gmail.com, hiranmaysamanta@gmail.com, poopoolee50@hotmail.com, sahahiran@gmail.com)

‡ Corresponding Author; First Author, CEGESS, IIEST, Shibpur Tel: +91 (033) 2668 4561,

Fax: +91 (033) 2668 2916, joydipjana02@gmail.com

Received: 19.02.2018 Accepted:17.04.2018

Abstract- This paper presents the design and development of a novel highly efficient synchronous buck converter operating both as a battery charge controller with five stage charging method and also as improved Maximum Power Point Tracker (MPPT) for operation in Solar Photovoltaic (PV) Systems. The algorithm regulates the duty cycle of the switching devices of the converter following a variable step size perturb and observe (P&O) MPPT technique. At the same time it provides precise control on the battery charging voltage and current according to five charging stages which is desirable for protection of battery health and maximizing charging rate. Thus the algorithm developed provides a combined solution for maximizing the transfer of solar electricity generated by the PV module(s) and also ensuring a long battery lifetime. Both these aspects, which are generally investigated separately earlier, are treated in an integrated fashion in this work. The work analyses in detail about the converter power loss as well as describes the development of MPPT technique and battery charging method used in the controller. A prototype of 1500W MPPT Charge Controller based on this algorithm has been designed, fabricated and tested. It shows satisfactory performance of the MPPT charge controller in terms of performance parameters i.e. converter efficiency, MPP tracking efficiency, MPP tracking time, fluctuation of PV operating point around MPP, input operating voltage range of the controller, independency of battery type as well as provision of temperature compensation.

Keywords MPPT, Multi-stage Battery Charging, Efficiency of converter, Battery Life Extension, Synchronous Buck Converter.

1. Introduction

Solar PV systems include storage batteries for providing electricity on demand, solar smoothing or peak shaving [1]. Suitable charge controller is needed for interfacing the solar PV module(s) with the battery bank which should protect the battery health and at the same time enable maximum power transfer from the solar PV module(s) to the battery [2, 3]. The job of these controllers is to charge battery efficiently by following a proper charge method while preventing battery overcharge and over-discharge ensuring long battery lifetime.

Further as the Maximum Power Point (MPP) of a solar PV array varies with irradiance and temperature the charge controllers for PV system has to perform one more job which is to track the MPP very fast and efficiently with low PV operating point fluctuation around the MPP under both static (fixed irradiation) and dynamic (rapidly changing irradiation) weather conditions. But both these aspects of battery charge controller for PV systems have generally been investigated independently in technical literature so far [4].

Various charging methods for batteries are reported in the literature: single stage, and multi-stage. The constant-current (CC), constant-voltage (CV) and on-off charging are good examples for single stage method, while the constant-current constant-voltage (CCCV) is a good example for multistage charging method. CC, CV and on-off method often present the problem of not fully charging the battery, and also not protecting from premature aging of batteries [5]. It has been shown in [6] that, the multi-stage charging is the most efficient method regardless of the battery type. Multi-stage charge controllers generally have three charging stages namely, bulk, absorption and float, some of which are CV and the rest are CC charging [7]. Two additional stages namely soft charging and equalization charging may be incorporated in the charge controller to enhance the battery life cycle and its performance over the charge and discharge periods.

For charging batteries using PV module(s) a variety of MPPT techniques have been developed as reported in [8 - 16]. These techniques can be categorized as (1) offline techniques that are dependent on solar cell models, (2) online techniques which do not specifically rely on modeling of the solar cell behavior and (3) hybrid methods which are a combination of the two aforementioned methods. But two primary issues associated with these techniques are "PV operating point fluctuation around the target MPP" and "speed of MPP tracking" [4].

This paper first provides a review of the traditional battery charge controllers pointing out their limitations. Algorithm for the new MPPT charge controller is then developed that resolves limitations of the traditional controllers. The new controller can charge four types of batteries, namely, Flooded Lead acid battery, Valve regulated lead acid (VRLA) or sealed lead acid battery, VRLA Gel battery and VRLA Absorbent glass mat (AGM) battery. It on one hand brings the battery to a full charge efficiently by five-stage charging ensuring long battery lifetime and on the other hand tracks the MPP very fast and efficiently with small PV operating point fluctuation around the MPP under both static and dynamic weather conditions by using a variable step size perturb and observe (P&O) MPPT technique. The efficiency of the converter used in the controller has been enhanced through some special means. Additionally the need to provide a very wide input voltage range in the charge controller has also been addressed in this work [17].

Various experimental tests have been performed in order to verify the performance of the new charge controller. The experimental results show that, the new controller has high converter efficiency. It can extract as much power as possible to charge the battery with a very high MPP tracking speed with small PV operating point fluctuation around the MPP and it has high static and dynamic MPP tracking efficiency.

2. Methodology

2.1. Five stage charging

Various controllers for charging batteries have been used over the past several decades in keeping with the substantial development in technologies from flooded lead acid batteries to VRLA batteries as reported in the literature [18 - 20]. Among them the CCCV controller has been the most commonly used [21]. A fast charging can be done with high charge rates and/or high voltage set points [22, 23]. However, on the whole, a fast charging has negative effect on battery aging factors like water loss, grid corrosion and sulfation of the negative electrode [21]. Furthermore, when fast charging of VRLA batteries is not appropriately controlled, significant harm may occur, eventually resulting in a reduced battery life. Charge control methods which minimize the battery life degradation can be achieved by putting constraints on the battery states such as charging current, the battery voltage, the state-of-charge and the battery temperature which are typically provided by the battery manufacturer [24 - 27]. However, such constraints are rather conventional as they are provided for the complete lifetime of the battery and are typically expected in three-stage CCCV charge controller [28]. But a problem arises in three-stage controllers which is as follows: if the battery condition is not good enough to accept high amount of current during bulk charging then low current should be applied before bulk stage only to make the battery healthy to accept high current charging. Soft charging is needed to overcome this limitation.

The last stage in a traditional three-stage charge controller is called the float stage where battery charging voltage is lowered than that of the previous stage and constant voltage is applied. If left in an extended float state, the battery faces the threat of acid sulfate *stratification*. Stratification occurs when the acid in the electrolyte mixture separates from the water and begins to concentrate at the bottom of the battery, reducing the performance and life of the battery. Thus an equalization charging is required to maintain a balance between battery overcharging and undercharging and to prevent battery stratification.

2.2. MPPT techniques

Researchers have given continuous efforts on the design and implementation of the MPPT techniques in PV system to attain improved performance parameters. The objectives are: increasing their speed of MPP tracking with small PV operating point fluctuation around the MPP and making them to be operated in both constant and rapidly varying weather conditions. In this section, the recent publications on the design and implementation of MPPT controllers used in PV system will be reviewed to show their main characteristics, and limitations. This would help us to enhance the performance parameters in maximizing the use of PV energy for battery charging.

A MPPT charge controller as described in [29] is a type of battery charge controller that ideally brings the operating point of a PV module to its MPP [30]. It is widely used in PV systems to increase their MPP tracking efficiency [31], and to extract the maximum possible instant power from the PV module [32]. Hill-climbing (HC) MPPT techniques include Perturb and Observe (P&O), Incremental Conductance (I&C), open-circuit voltage (OCV), short-circuit current (SCC), Extremum Seeking Control (ESC) etc. which are discussed in detail in [33 - 44]. Some artificial intelligence MPPT techniques such as artificial neural network (ANN), fuzzy logic control (FLC) etc. and MPPT technique iterative in nature such as genetic algorithm (GA) are discussed in [45 - 47]. Two primary parameters associated with these MPPT techniques are "PV operating point fluctuation around the target MPP" and "speed of MPP tracking" and there is a tradeoff between these two parameters which need to be considered. In table 1, the MPP tracking time and the operating point fluctuation around the MPP for different MPPT techniques have been presented.

Table 1. MPP tracking time and operating point fluctuation around target MPP for different MPPT techniques

MPPT technique	MPP tracking time	Operating point fluctuation around the target MPP
stand-alone FLC [48]	27 ms	2%
combination of ANN and P&O [49]	2 ms	nil
combination of ANN and I&C [50]	40 ms	-
combination of ANN and GA [51]	-	1.45%
GA optimized FLC [52]	715 ms	0.02%
HPNN coupled with FLC [53]	10-40 ms	0.002%
standalone FLC [54]	150 ms	-
FLC integrated with HC [55]	70 ms	-
adaptive fuzzy logic control [56]	3 ms	-
second order sliding mode-based MPPT [57]	0.2 s	-

It has to be noted that, amongst all the above-mentioned MPPT techniques, none are implemented in hardware, and hence their practical feasibility could not be established.

3. Developed Charge Controller

As discussed previously, the limitations of the traditional controllers are premature ageing, slow MPP tracking speed, large PV operating point fluctuation around the target MPP, low static and dynamic MPP tracking efficiency. All these limitations have been overcome in the newly developed controller. The converter efficiency has also been improved. Beside these some aspects such as battery type dependency, incompatibility with large range of input PV voltage, temperature compensation etc. have also been addressed. Moreover, as discussed earlier two additional stages namely soft charging and equalization charging have been applied in the developed controller along with the three existing stages of traditional controller to achieve balance between battery overcharging and undercharging and to prevent battery stratification. The next sections present the design, implementation, and validation of the developed charge controller showing how it successfully resolves the limitations of the traditional controllers.

3.1. Synchronous buck converter

A prototype of the charge controller has been developed which is a synchronous DC-DC buck converter of 1500W power transferring capacity (fig. 1). A solid state relay has been used in parallel with the reverse polarity protection power diode as shown in Fig. 1., which bypasses the diode above a certain delivering power to minimize the power loss across the diode as the voltage drop of the diode is high.

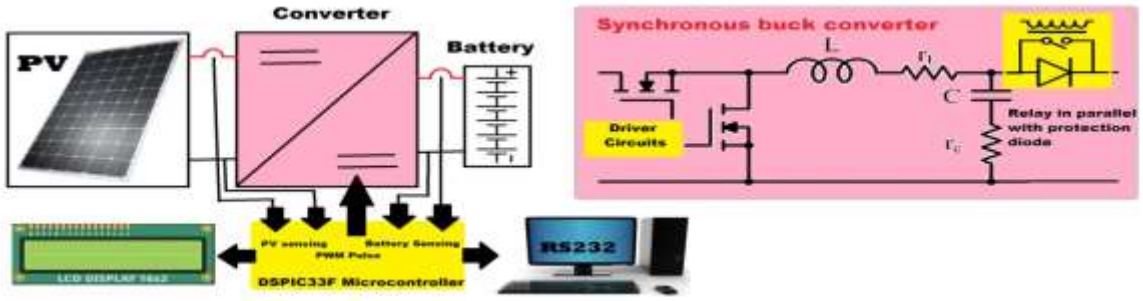

Fig. 1. Circuit diagram of the controller with synchronous buck converter

The hardware of the prototype is composed of four main sections, namely the power section consisting of power switching devices with their driver circuits, the control section, the sensing section and the display. The control section contains a DSPIC33F microcontroller. The main function of this section is to generate the PWM pulses with variable duty following MPPT technique, which drive switching devices of the DC-DC converter using the driver

circuits. The sensing section contains several sensors and their peripheral circuit components. It comprises the negative temperature co-efficient thermocouple for temperature sensing, resistive voltage divider based sensors for PV and battery voltage measurement and hall based current sensors for PV and battery current measurements. The hardware also contains a 16*2 LCD to display various charging parameters.

As power loss analysis of the converter is important for converter design optimization following efficiency enhancement major component loss of synchronous buck converter used in the prototype have been described as follows [58]:

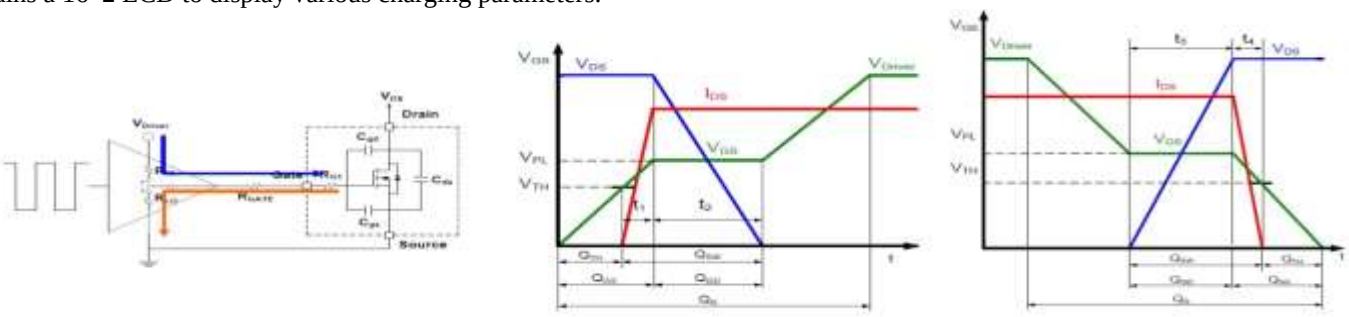

Fig. 2. (a) Device driver turns on and off path, (b) Device driver on, (c) Device driver off

Fig. 2 shows the device driver turn on and off path respectively, whereas fig. 3 shows the high-side and low-side device conduction on respectively.

The high-side device's switching on loss is [58],

$$P_{hs\_on} = f_{SW} \times V_{DS} \times I_{DS} \times \frac{t_1+t_2}{2} = f_{SW} \times V_{in} \times I_{out} \times \frac{T_{hs\_on}}{2} \quad (1)$$

Where, $\frac{T_{hs\_on}}{2} = \frac{Q_{SW}}{I_{G\_on}}$ and $I_{G\_on} = \frac{V_{driver} - V_{PL}}{R_{HI} + R_G + R_{G1}}$ (2)

The conduction loss of high-side switching device is determined by the on-resistances of the device and the device RMS current which is as follows:

$$P_{con\_hs} = I_{RMS\_HG}^2 \times R_{DS\_on\_hs} \quad (3)$$

Where, $I_{RMS\_HS} = \sqrt{D \times (I_{out}^2 + \frac{I_{ripple}^2}{12})}$ (4)

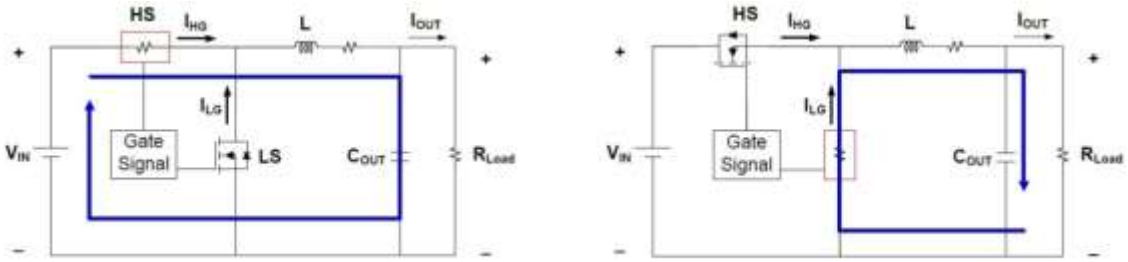

Fig. 3. (a) High-side device conduction on, (b) Low-side device conduction on

The conduction loss of low-side switching device is as follows,

$$P_{con\_ls} = I_{RMS\_LG}^2 \times R_{DS\_on\_ls} \quad (5)$$

Where, $I_{RMS\_LG} = \sqrt{(1-D) \times (I_{out}^2 + \frac{I_{ripple}^2}{12})}$ (6)

The dead-time loss induced by low-side device body diode conduction during dead-times is as follows,

$$P_{deadtime} = V_{SD} \times [\left(I_{out} - \frac{I_{ripple}}{2}\right) \times T_{D2} + (I_{out} + \frac{I_{ripple}}{2}) \times T_{D1}] \times f_{SW} \quad (7)$$

And the low-side device reverse recovery charge loss is as follows,

$$P_{rr} = Q_{rr} \times V_{DD} \times f_{SW} = Q_{rr} \times V_{in} \times f_{SW} \quad (8)$$

3.1.1. Improving maximum power point tracking

The controller employs P&O MPPT technique with some modifications to improve the tracking speed of MPP and to lower the PV operating point fluctuations around MPP. An important reason of selecting P&O technique is that it is not PV module size dependent and the controller has to provide a very wide input voltage range with which it can make use of broad range of PV modules. The duty cycle of the switching

device in the converter is set according to the requirement of the PV voltage perturbation step size and it varies to balance between two conflicting parameters, namely the speed of MPP tracking and the fluctuation of the PV operating point around the MPP. When the controller starts the MPP tracking process, it executes a dynamic pilot loop program which basically traverse the I-V characteristics curve of the PV module from the open circuit point towards the MPP. In dynamic MPPT loop, PV voltage is perturbed with big step size to catch the MPP fast as shown in Fig. 4. The dynamic MPPT loop also is applied in that situation when there is a big change in PV power generation or the irradiation is changing very fast.

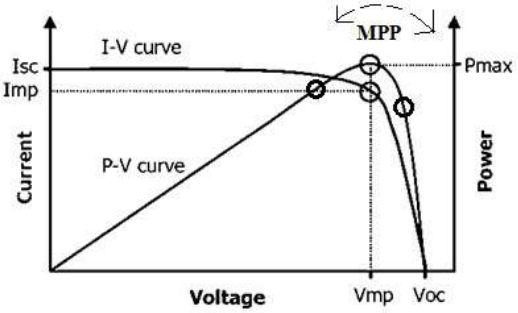

Fig. 4. Fluctuation of operating point around MPP with big step size of PV voltage perturbation

In dynamic MPPT loop the step size of PV voltage perturbation is high leading to fluctuation of the PV operating point around the MPP. Once the controller catches the MPP, then static MPPT loop is applied where the step size of the PV voltage perturbation becomes small to attain low fluctuation of the PV operating point around the MPP which has been shown in Fig. 5. And when there is no change in irradiation or there is a slow change in irradiation, then also the static MPPT loop is applied. This is the main idea of performance optimization between the tracking speed of MPP and the PV operating point fluctuations around MPP. Now until there is a big power change due to sudden fast change of solar irradiation the program loop stays in this static MPPT and it stays here very stable with high static MPP tracking efficiency due to small step size of the PV voltage perturbation. A look up table (LUT 1) has been prepared and incorporated in the microcontroller program used in the control section of the charge controller as shown in Table 2 where the set points of power change due to irradiation change according to the power delivery from PV module to the battery have been given. The static and dynamic loops swing between each other when there is a change of power equal to this set value. For example, if the controller is delivering power of 500W to the battery, then the set point for power change is 0.5W i.e. if there is a power change of 0.5W then it goes from static loop to dynamic loop to catch the new MPP quickly by increasing the step size of PV voltage perturbation.

Table 2. The set points of power change according to the power delivery (LUT 1)

Power delivery	Set point of power change
500W	0.5W
1000W	1W
1500W	1.5W

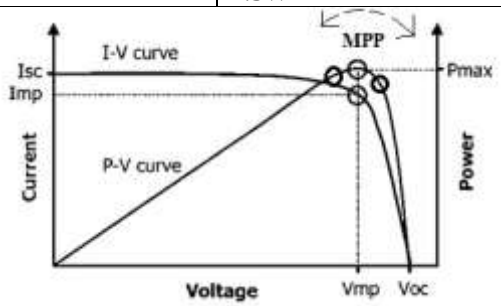

Fig. 5. Fluctuation of operating point around MPP with small step size of PV voltage perturbation

3.2. Multi-stage charging

The stages incorporated in the developed controller are soft charging, bulk charging, absorption charging, float charging and equalization stage respectively. The set voltage in each and every charging stage for each of the batteries have been prepared and incorporated in the microcontroller program of the new charge controller. The flow chart of the charging method and the charging current and voltage curves have been shown in Fig. 6(a) and Fig. 6(b) respectively. In case of VRLA Gel batteries and VRLA AGM batteries the equalization stage has been neglected. The developed controller detects battery state-of-charge by detecting battery voltage prior to charging. After reading the battery voltage the controller determines which stage to properly charge at. In Table 3, the open circuit voltage (OCV) for different state-of-charge (SOC) for different types of batteries has been shown. In Table 4, the type of charging whether it is constant current charging or constant voltage charging and the state of the charge for each charging stage has been shown. In Table 5, voltage level or state-of-charge in different charging stages have been shown for four types of batteries. The controller slightly changes the voltage set points for every stage according to the change of temperature and in this way the temperature is compensated. A look up table (LUT 2) has been prepared and incorporated in the microcontroller program of the charge controller to determine the PV voltage set points with increase/decrease rate of voltage for temperature change which has been shown in Table 6 for different types of batteries.

Table 3. The open circuit voltage (OCV) for different state-of-charge (SOC) for different types of batteries

Battery type	Open circuit voltage (OCV) @20% state-of-charge	Open circuit voltage (OCV) @50% state-of-charge	Open circuit voltage (OCV) @60% state-of-charge	Open circuit voltage (OCV) @70% state-of-charge	Open circuit voltage (OCV) @90% state-of-charge

	(SOC)	(SOC)	(SOC)	(SOC)	(SOC)
Flooded lead acid battery	-	49.76V	50.08V	50.4V	51.08V
Sealed lead acid battery or VRLA	48.4V	49.76V	50.08V	50.4V	51.08V
VRLA Gel battery	48V	49.6V	50.0V	50.4V	51.96V
VRLA AGM battery	48V	49.6V	50.0V	50.4V	51.96V

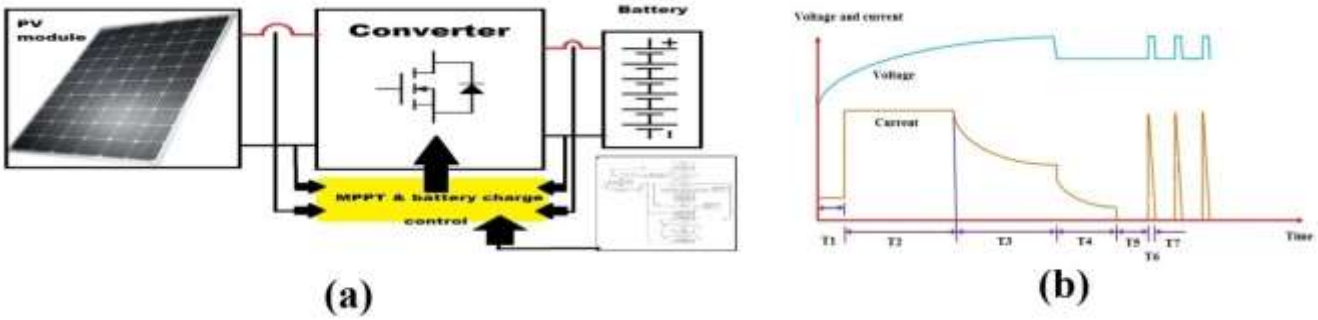

Fig. 6. (a) Flowchart of the battery charging method, (b) Five stage battery charging in the developed controller

Table 4. The type of charging and the state of the charge for each charging stage

Charging stage	Type of charging	State-of-charge
Soft(T1)	Constant current charging with C(capacity)/100 current	Up to 20% state-of-charge (V_{Soft})
Bulk(T2)	Constant current charging with C(capacity)/10 current	20%-80% state-of-charge (V_{Bulk})
Absorption(T3)	Constant voltage charging	80%-100% state-of-charge ($V_{Absorption}$)
Float(T4)	Constant voltage charging	V_{Float}
Equalization (T5)	No charging	-

Table 5. Voltage level of different types of battery in different charging stages

Charging stage	Battery type			
	Flooded lead acid battery	Sealed lead acid battery or VRLA	VRLA Gel battery	VRLA AGM battery
Soft(T1)	54V	53.6V	51.2V	51.2V
Bulk(T2)	59.2V	58.8V	56.4V	56.4V
Absorption(T3)	60.0V	59.6V	57.6V	57.6V
Float (T4)	54V – 55.2V	52.8V – 53.6V	54V – 55.2V	54.4V – 55.2V
Equalization(T5)	Charge voltage on point – 50.4V Charge voltage off point – 54V	Charge voltage on point – 50.4V Charge voltage off point – 52.8V	Charge voltage on point – 51V Charge voltage off point – 54V	Charge voltage on point – 51V Charge voltage off point – 54.4V

The first charging stage is soft charging which is constant current charging. This stage has been applied only when the battery state-of-charge is below 20% or the battery voltage is lower than V_{Soft}. As in bulk charging stage, battery is charged with a high current and if the battery state-of-charge is lower than 20% then the battery is not capable to accept this high current. In this stage if the PV module voltage is greater than the minimum input operating voltage of the controller then PV module charges the battery with C/100 (C = Capacity of the battery in AH) current up to 20% state-of-charge. The next three charging stages named bulk, absorption, and float are same as those of traditional charge controllers. As shown in Fig. 6(b), T1, T2, T3, T4 signifies the soft, bulk, absorption, and float charging stages respectively and T5 and T6 denotes the charge on period and charge off period during equalization stage respectively which has been discussed next.

Table 6. Temperature compensation for different types of batteries (LUT 2)

Battery type	Temperature compensation
Flooded lead acid battery	For average operating temperatures below this range (colder than) or above this range the maximum voltage set point should be compensated with an increase or with a decrease at a rate of 0.063 Volts Per Cell (1.512V Volts for a 48V battery) for every 10ºC.
Sealed lead acid battery or VRLA	1.512V Volts for a 48V battery for every 10ºC.
VRLA Gel battery	1.2V Volts for a 48V battery for every 10ºC.
VRLA AGM battery	0.432V Volts for a 48V battery for every 10ºC.

The last stage is the equalization charging stage. In this stage, the developed controller monitors if the battery has remained in the float stage for a specified length of time or if the battery voltage drops below a minimum level. The charge controller then enters this stage by automatically initiating a new round of charging, correcting the undercharge condition and stimulating the mixing of the electrolyte solution. Specifically, the equalization stage of the developed controller automatically repeats the charge cycle every seven days or when the battery voltage drops below a determined voltage as shown in Fig. 7. By using this technique, a balance is achieved between overcharging and undercharging and stratification is prevented. The construction of AGM and Gel batteries eliminates any stratification, thus this stage has not been applied in these batteries. After equalization stage the charge controller goes to the bulk charging stage and repeats the whole charging cycle.

4. Experimental Result

An experimental setup has been prepared as shown in Fig. 7 (b) in order to experimentally test the new controller (shown in Fig. 7 (a)), and to work out on its main MPPT performance parameters, two modes of operation have been arranged and examined. The first mode, when the controller has been operated with fixed irradiation condition to find out its static MPP tracking efficiency. The second mode, when it has been operated with varying irradiation condition to find out its dynamic MPP tracking efficiency. A TerraSAS make PV simulator has been used instead of original PV module for charging a battery bank of 48V nominal voltage. Different types of PV modules (Operating temperature: -40˚C to +85˚C, Temperature Co-efficient for Voc/˚C (B): -0.34%, Temperature Co-efficient for Isc/˚C (a): 0.05%, Temperature Co-efficient for power/˚C (y): -0.43%) can be used to charge batteries using this new controller and the controller has been tested with these PV module parameters settings in the PV simulator which have been shown in Table 7. For voltage and current measurement of PV module and battery, a Yokogawa make power meter (model: WT330) has been used in this experimental set-up. The gate signals (captured in oscilloscope) applied to the high-side and low-side devices have been shown in fig. 8.

Fig. 7. (a) The developed charge controller, (b) Experimental set-up

Table 7. Parameters of the PV modules can be used for this controller

Parameter	Value							
Peak power	150W	205W	250W	300W	305W	310W	315W	320W
Voltage at peak power, Current at peak power	36.22V, 4.15A	36.18V, 5.67A	36.18V, 6.92A	36.14V, 8.31A	36.30V, 8.41A	36.40V, 8.52A	36.49V, 8.64A	36.56V, 8.76A
Open circuit voltage, Short circuit current	44.46V, 4.37A	44.41V, 5.97A	44.46V, 7.28A	44.46V, 8.74A	44.60V, 8.82A	44.71V, 8.92A	44.86V, 9.01A	45.01V, 9.11A
Module efficiency (%)	15.21%	14.09%	15.53%	15.63%	15.89%	16.15%	16.41%	16.67%

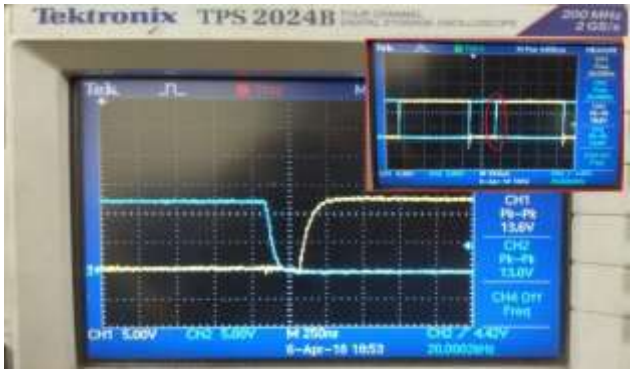

Fig. 8. Gate signals of the high-side and low-side device

4.1. Mode I: Static MPPT performance test

In this mode, the irradiation has been fixed at 120 W/m^2 and the temperature has been fixed at 25˚C in the PV simulator. Fig. 9, 10 and 11 represent the output voltage, current and power curve of the PV with respect to time indicated in blue together with the ideal response indicated in black. In these experiments, sixty numbers of data points have been recorded using the power meter used in the experimental set up in a second for each parameter. According to Fig. 11, it takes 1 second for the developed controller to reach the MPP and there a fluctuation of 0.86% around the target MPP has been achieved.

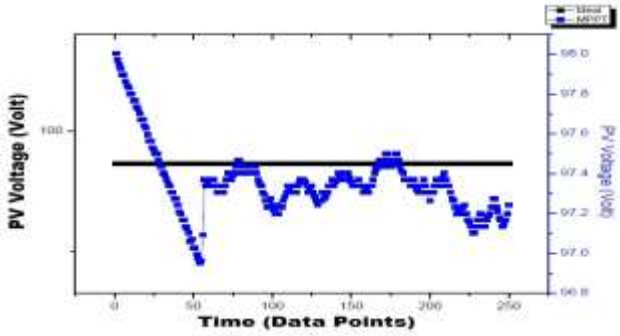

Fig. 9. The output voltage of the PV with respect to time while charging in static irradiation condition

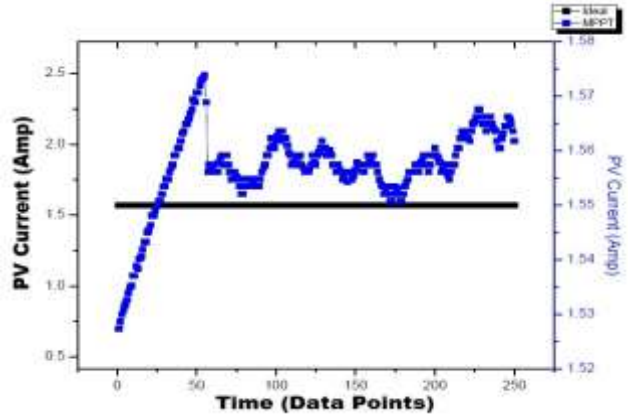

Fig. 10. The output current of the PV with respect to time while charging in static irradiation condition

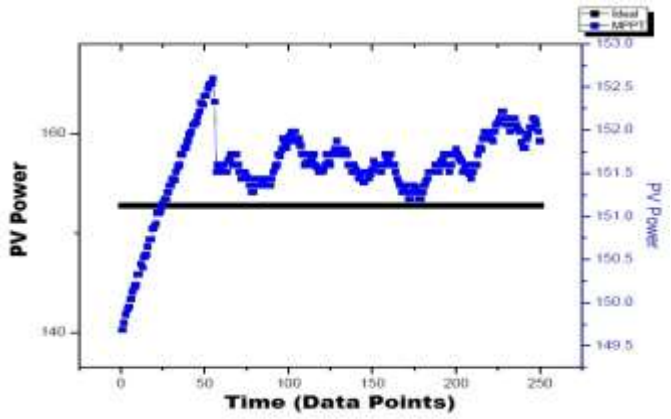

Fig. 11. The output power of the PV with respect to time while charging in static irradiation condition

4.2. Mode II: Dynamic MPPT performance test

In this mode, the irradiation has been varied in the PV simulator according to the dynamic irradiation profile shown in Fig. 12. According to this dynamic profile the irradiation has been varied from 100 $W/m^2$to 1000 W/m^2 and some time the change of irradiation is so fast that it has been found very close to step jump of irradiation change.

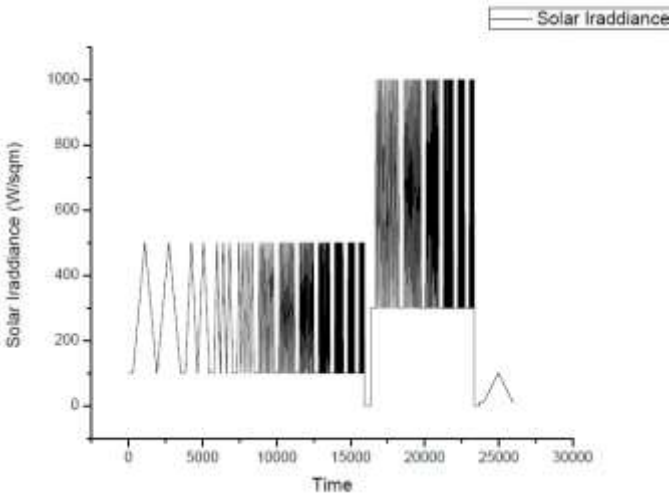

Fig. 12. Dynamic irradiation profile used in the experiment

To find out the dynamic MPP tracking efficiency of the new controller, some portions of the full dynamic response has been zoomed in, which have been shown in Fig. 13, Fig. 14. and Fig. 15. Fig. 13 demonstrates that when the irradiation changes from 257 W/m^2 to 255 W/m^2, then the controller takes only 1.67 second to find the new MPP and when it catches the new MPP the fluctuation has been found 0.5% around the new MPP.

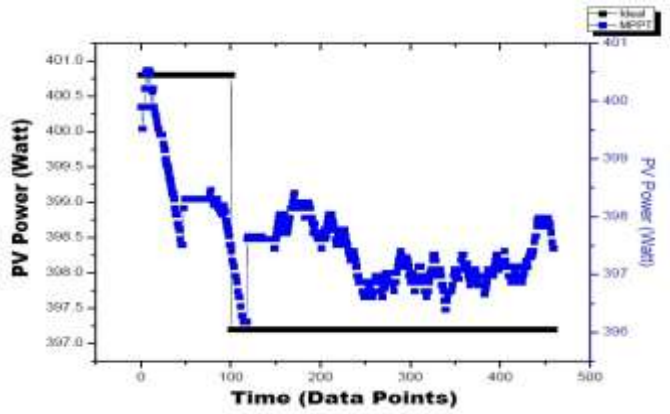

Fig. 13. PV power in the dynamic condition (when the irradiation changes from 257 W/m^2 to 255 W/m^2

In Fig. 14, the PV current and MPP tracking efficiency according to the dynamic response of the controller have been shown where the irradiation has a nature of ramp up from 100 W/m^2 to 500 W/m^2 first and then a ramp down from 500 W/m^2 to 100 W/m^2. It has been seen from the figure that the shape of changing the PV current follows the shape of the irradiation.

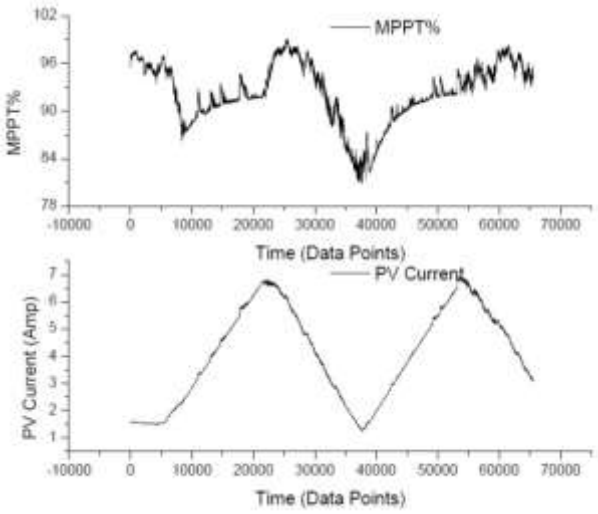

Fig. 14. MPP tracking efficiency and PV current in dynamic condition (when the irradiation changes from 100 W/m^2 to 500 W/m^2)

In Fig. 15, the MPP tracking efficiency has been shown where the irradiation has a nature of ramp down from 500 to 100 W/m^2. The figure shows that the minimum dynamic MPP tracking efficiency i.e. MPP tracking efficiency in varying irradiation condition has been found 96.5% and the maximum dynamic MPP tracking efficiency has been found 98.5% during the whole MPP tracking process according to the irradiation change.

4.3. Converter efficiency test

To find out the converter efficiency of the developed controller for minimum load condition to full load condition, three sets of operation have been arranged and examined. The first set, when the controller has been operated with a PV configuration of V_{oc}= 85V in the TerraSAS PV simulator.

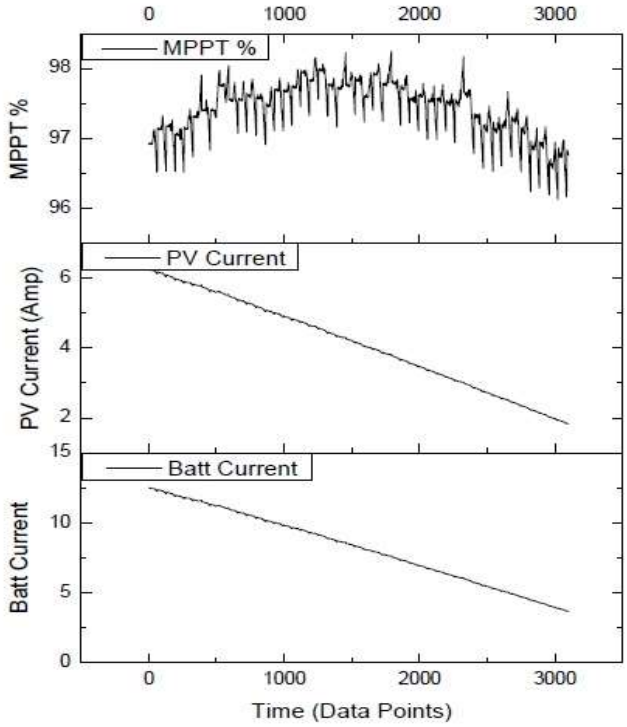

Fig. 15. MPP tracking efficiency and PV and battery charging current in dynamic condition (when the irradiation changes from 100 $W/m^2$to 500 W/m^2)

The second set, when the controller has been operated with a PV configuration of V_{oc}= 115V in the PV simulator. The last set, when the controller has been operated with a PV configuration of V_{oc}= 135V in the PV simulator. In each set of operation the irradiation has been set in the PV simulator at that level which is required for generating output power according to the load percentage and the PV and battery parameters reading have been noted down to calculate the conversion efficiency. Beside the job of finding the conversion efficiency, the MPP tracking efficiency has also been noted down during this whole experimental operation.

Table 8. Tested @ 85V (Battery voltage less than 50V and temperature 25^oC)

SL No.	Load%	5%	10%	25%	50%	75%	100%
1	Battery Voltage (V)	48.1	48.2	48.4	48.8	49.2	49.7
2	Battery Current (A)	1.33	2.92	7.49	14.88	21.98	29.88
3	Battery Power (W)	64.3	140.7	362.8	726.1	1081.33	1484.9

4	PV Voltage (V)	71.3	72.9	74.7	76.4	78.0	79.6
5	PV Current (A)	1.0	2.0	4.9	9.6	14.1	19.3
6	PV Power (W)	68.6	144.2	367.3	733.4	1097.8	1532.3
7	Converter efficiency (%)	93.8	97.6	98.8	99.0	98.5	97.5
8	MPP tracking efficiency (%)	95.7	96.8	98.8	99.2	98.6	97.5

Table 9. Tested @ 115V (Battery voltage less than 50V and temperature 25°C)

SL No.	Load%	5%	10%	25%	50%	75%	100%
1	Battery Voltage (V)	48.2	48.3	48.5	49.0	49.3	49.7
2	Battery Current (A)	1.69	3.0	7.48	16.37	22.54	28.94
3	Battery Power (W)	81.8	145	362.85	802.2	1111.7	1438.4
4	PV Voltage (V)	96.4	95.5	100.1	112.1	101.6	103.1
5	PV Current (A)	0.9	1.6	3.7	7.3	11.2	14.2
6	PV Power (W)	86.9	149.8	369.5	816.9	1135.6	1469.3
7	Converter efficiency (%)	94.2	96.8	98.2	98.2	97.9	97.9
8	MPP tracking efficiency (%)	97.9	98.3	98.6	99.7	99.9	99.7

Table 10. Tested @ 135V (Battery voltage less than 50V and temperature 25°C)

SL No.	Load%	5%	10%	25%	50%	75%	100%
1	Battery Voltage (V)	48.4	48.5	48.8	49.1	49.5	49.9
2	Battery Current (A)	1.5	3.14	7.91	15.49	23.26	30.03
3	Battery Power (W)	72.8	152.6	386.12	760.36	1151.19	1498.3
4	PV Voltage (V)	106.4	116.8	120.9	128.6	125.4	127.8
5	PV Current (A)	0.7	1.3	3.2	6.0	9.4	12.1
6	PV Power (W)	76.6	156.8	392.4	774.3	1179.5	1544.7
7	Converter efficiency (%)	95	97.3	98.4	98.2	97.6	97
8	MPP tracking efficiency (%)	95.9	98.1	99.5	98.3	98.2	99.7

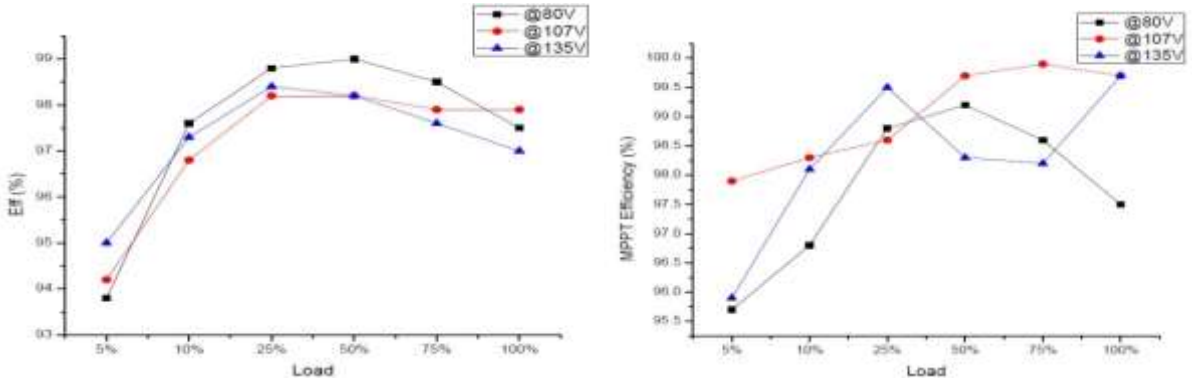

Fig. 16. (a) Converter efficiency curve for different load condition, (b) MPP tracking efficiency curve for different load condition .

It has been observed from Fig. 16(a), that the maximum converter efficiency of the controller has been found 99%. In Table 8, 9 and 10, the PV operating voltage for different loading condition has been shown and it is found that the new controller is operating in a wide input voltage range i.e. 71.3V – 127.8V. And in Fig. 16(b), the MPP tracking efficiency for different loading condition has been shown and it is found that the highest MPP tracking efficiency has been found 99.9%.

5. Conclusion

This paper briefly reviews the limitations of the existing charge controllers which are mostly three stage chargers and MPPT techniques reported so far with regard to battery charging for solar PV systems. The design and implementation of a new controller, which is a combined solution of a five-stage battery charging and an efficient MPPT technique is proposed in this paper. Two additional stages included in the controller namely, the soft charging and the equalization charging with the three existing stages of traditional controllers ensures a balance between battery overcharging and undercharging and prevent battery stratification

resulting in a longer battery life. The controller employs an improved P&O algorithm with variable duty cycle for fast MPP tracking and very low PV operating point fluctuation around the MPP, and high static and dynamic MPP tracking efficiency. Important issues like design of chargers and MPPT for different voltage set points for overcharging and deep discharge cutoff for different types of battery like Lead acid battery i.e. whether Flooded, Valve regulated (VRLA) or sealed VRLA Gel battery and VRLA Absorbent glass mat (AGM) battery have been taken into account, analyzed and solved. Also the incompatibility issues like large range of input PV voltage and temperature variation has been investigated and solved.

The experimental results show that, the new controller has maximum converter efficiency of 99%, and it can extract as much power as possible to charge the battery with a MPP tracking speed of 1 second and maximum MPP tracking efficiency of 99.9% with a fluctuation of 0.86% around the target MPP in static irradiation condition. And in dynamic irradiation conditions the before mentioned performance parameters become 1.67 second, 98.5% and 0.50% respectively. The controller has a very wide input voltage range of 71.3V – 127.8V with which it can be coupled to a wide range of PV modules available in today's market for charging batteries in the PV application.

Acknowledgements

This work was supported by Ministry of New and Renewable Energy (MNRE), Government of India (IIESTS Project Code: - DRC/MNRE/CEGESS/HS/006/11-12).

References

[1] M. Chiandone , C. Tam, R. Campaner , G. Sulligoi, "Electrical storage in distribution grids with renewable energy sources. In: International Conference on Renewable Energy Research and Applications (ICRERA)", 2017.

[2] Desconzi, M., Beltrame, R., Rech, C., Schuch, L., Hey, H., "Photovoltaic standalone power generation system with multilevel inverter", *In:International Conference on Renewable Energies and Power Quality (ICREPQ*), Las Palmas, Spain, April.

[3] Jana J, Bhattacharya KD, Saha H. Design & implementation of MPPT algorithm for battery charging with photovoltaic panel using FPGA, 2014. *In: Power India International Conference (PIICON)*, 10.1109/POWERI.2014.7117704.

[4] Reisi Ali Reza, Morad Moha00mmad Hassan, Jamasb Shahriar, "Classification and comparison of maximum power point tracking techniques for photovoltaic system: a review". *Renew Sustain Energy Rev* 2013:475–88.

[5] Hirech, K., Melhaoui, M., Yaden, F., Baghaz, E., Kassmi, K., "Design and realization of an autonomous system equipped with a charge/discharge regulator and digital MPPT command". *Energy Proc.* 42, 503–512.

[6] Pamela G. Horkos, Emile Yammine, Nabil Karami, "Review on Different Charging Techniques of Lead-Acid Batteries", 10.1109/TAEECE.2015.7113595.

[7] Md Shahrier Hakim, Farhana Latif, Md. Imran Khan, Al Basir, "Design and implementation of three-stage battery charger for lead-acid battery", 10.1109/CEEICT.2016.7873052.

[8] Salas V., E. Olı´as, A. Barrado, A. La´zaro, "Review of the maximum power point tracking algorithms for stand-alone photovoltaic systems", *Solar Energy Materials & Solar Cells* 90, 1555–1578.

[9] Esram T., Kimball J. W., Krein P. T., Chapman P. L., Midya P., "Dynamic maximum power point tracking of photovoltaic arrays using ripple correlation control", *IEEE Trans. Power Electron.*, vol. 21, no. 5, pp. 1282–1291.

[10] Kazuhiro Kajiwara, Nobumasa Matsui, Fujio Kurokawa, "A new MPPT control for solar panel under bus voltage fluctuation. In: International Conference on Renewable Energy Research and Applications (ICRERA)", 2017.

[11] S.A. Rizzo, N. Salerno, G. Scelba, A. Sciacca, "Enhanced Hybrid Global MPPT Algorithm for PV Systems Operating under Fast-Changing Partial Shading Conditions", Internatıonal Journal of Renewable Energy Research, 2018 Vol. 8, No. 1.

[12] Xingshuo Li, Huiqing Wen, Yihua Hu, "Evaluation of different maximum power point tracking (MPPT) techniques based on practical meteorological data. In: International Conference on Renewable Energy Research and Applications (ICRERA)", 2016.

[13] Neeraj Priyadarshi, Amarjeet Kumar Sharma, S Priyam, "Practical Realization of an Improved Photovoltaic Grid Integration with MPPT", Internatıonal Journal of Renewable Energy Research, 2017, Vol. 7, No. 4.

[14] A. Dolara, S. Leva, G. Magistrati, M. Mussetta, E. Ogliari, R. Varun Arvind, "A novel MPPT algorithm for photovoltie systems under dynamic partial shading — Recurrent scan and track method. In: International Conference on Renewable Energy Research and Applications (ICRERA)", 2016.

[15] Neeraj Priyadarshi, Amarjeet Kumar Sharma, Faarooque Azam, "A Hybrid Firefly-Asymmetrical Fuzzy Logic Controller based MPPT for PV-Wind-Fuel Grid Integration", Internatıonal Journal of Renewable Energy Research, 2017, Vol. 7, No. 4.

[16] G. Graditi, G. Adinolfi, A. Del Giudice, "Experimental performances of a DMPPT multitopology converter. In: International Conference on Renewable Energy Research and Applications (ICRERA)", 2015.

[17] Julio López, S.I. Seleme Jr., P.F. Donoso, L.M.F. Morais, P.C. Cortizo, M.A. Severo, "Digital control strategy for a buck converter operating as a battery charger for stand-alone photovoltaic systems". *Sol. Energy* 140, 171–187.

[18] Reddy T. Linden, 2010. Reddy T. Linden's handbook of batteries. 4th ed. *McGraw-Hill Education*; 2010.
[19] Parker DAJ, Moseley PT, Garche J, Parker CD, "Valve-regulated lead-acid batteries". *Amsterdam: Elsevier*; 2004.
[20] Hunter PM, "VRLA battery float charge: analysis and optimization". Christchurch, New Zealand: University of Canterbury; 2003.
[21] Wong Y, Hurley W, Wölfle W, "Charge regimes for valve-regulated lead-acid batteries: performance overview inclusive of temperature compensation". *J Power Sources* 2008;183(2):783–91.
[22] Valeriote EM, Nor J, Ettel VA. "Very fast charging of lead-acid batteries". In: Proceedings of the 5th international lead-acid battery seminar, *International Lead Zinc Research Organization (ILZRO)*. p. 93–122.
[23] Fleming F, Shumard P, Dickinson B, "Rapid recharge capability of valve regulated lead-acid batteries for electric vehicle and hybrid electric vehicle applications". *J Power Sources* 1999;78(1):237–43.
[24] Hunter PM, Anbuky AH. "VRLA battery rapid charging under stress management". *IEEE Trans Industr Electron* 2003;50(6):1229–37.
[25] Jones RH, McAndrews JM, Vaccaro F, "Recharging VRLA batteries for maximum life. In: Twentieth international telecommunications energy conference", 1998. *INTELEC. IEEE; 1998*. p. 526–31.
[26] Li Y, Chattopadhyay P, Ray A, "Dynamic data-driven identification of battery state-of-charge via symbolic analysis of input–output pairs". *Appl Energy* 2015;155:778–90.
[27] Boisvert É, "Using float charging current measurements to prevent thermal runaway on VRLA batteries". *In: Twenty-third international telecommunications energy conference, 2001. INTELEC 2001. IET*; 2001. p. 126–31.
[28] Klein R, Chaturvedi NA, Christensen J, Ahmed J, Findeisen R, Kojic A, "Optimal charging strategies in lithium-ion battery. In: American Control Conference (ACC)", 2011. IEEE; 2011. p. 382–7.
[29] Fathabadi H, "Lambert W function-based technique for tracking the maximum power point of PV modules connected in various configurations". *Renewable Energy* 2015;74:214–26.
[30] Tsang KM, Chan WL, "Model based rapid maximum power point tracking for photovoltaic systems". *Energy Convers Manage* 2013;70:83–9.
[31] Tsang KM, Chan WL, "Three-level grid-connected photovoltaic inverter with maximum power point tracking". *Energy Convers Manage* 2013;65:221–7.
[32] Ammar MB, Chaabene M, Chtourou Z, "Artificial Neural Network based control for PV/T panel to track optimum thermal and electrical power". *Energy Convers Manage* 2013;65:372–80.
[33] Abdelsalam AK, Massoud AM, Ahmed S, Enjeti PN, "High-performance adaptive perturb and observe MPPT technique for photovoltaic-based microgrids". *IEEE Trans Power Electron* 2011;26(4):1010–21.
[34] Brunton SL, Rowley CW, Kulkarni SR, Clarkson C, "Maximum power point tracking for photovoltaic optimization using ripple-based extremum seeking control". *IEEE Trans Power Electron* 2010;25(10):2531–40.
[35] Dileep G. , S.N. Singh, "Application of soft computing techniques for maximum power point tracking of SPV system", *Sol. Energy* 141, 182– 202.
[36] Enslin JHR, Wolf MS, Snyman DB, Swiegers W, "Integrated photovoltaic maximum power point tracking converter". *IEEE Trans Ind Electron* 1997;44:769–73.
[37] Hiyama T, Kitabayashi K, "Neural network based estimation of maximum power generation from PV module using environmental information". *IEEE Trans Energy Convers* 1997;12:241–7.
[38] Jiang JA, Huang TL, Hsiao YT, Chen CH, "Maximum power tracking for photovoltaic power systems". *J Sci Eng* 2005;8(2):147–53.
[39] Lei P, Li Y, Seem JE, "Sequential ESC-based global MPPT control for photovoltaic array with variable shading". *IEEE Trans Sustain Energy* 2011;2(3):348–58.
[40] Liu F, Duan S, Liu F, Liu B, Kang Y, 2008. A variable step size INC MPPT method for PV systems. IEEE Trans Ind Electron 2008;55(7):2622–8.
[41] Masoum MAS, Dehbonei H, Fuchs EF, "Theoretical and experimental analyses of photovoltaic systems with voltage and current-based maximum power-point tracking". *IEEE Trans Energy Convers* 2002;17(4):514–22.
[42] Mei Q, Shan M, Liu L, Guerrero JM, "A novel improved variable step-size incremental-resistance MPPT method for PV systems". *IEEE Trans Ind Electron* 2011;58(6):2427–34.
[43] Noguchi T, Togashi S, Nakamoto R, 2002. Short-current pulse-based maximumpower-point tracking method for multiple photovoltaic-and-converter module system. IEEE Trans Ind Electron 2002;49(1):217–23.
[44] Park M, In-Keun Yu, "A study on the optimal voltage for MPPT obtained by surface temperature of solar cell". *In: 30th annual conference of IEEE* 3; 2004. p. 2040–5.
[45] Algazar MM, AL-monier H, EL-halim HA, El Kotb Salem ME, "Maximum power point tracking using fuzzy logic control". *Int J Electr Power Energy Syst* 2012;39 (1):21–8.
[46] Guenounou O, Dahhou B, Chabour F, 2014. Adaptive fuzzy controller based MPPT for photovoltaic systems. Energy Convers Manage 2014;78:843–50.
[47] Mellit A, Sağlam S, Kalogirou SA, "Artificial neural network-based model for estimating the produced power of a photovoltaic module". *Renewable Energy* 2013;60:71–8.
[48] Bazzi AM, Krein PT, "Concerning maximum power point tracking for photovoltaic optimization using ripple-based extremum seeking control". *IEEE Trans Power Electron* 2011;26(6):1611–2.

[49] Alabedin, A.M.Z., El-Saadany, E.F., Salama, M.M.A., "Maximum power point tracking for photovoltaic systems using fuzzy logic and artificial neural networks". *In: Power and Energy Society General Meeting. IEEE*, pp. 1–9.

[50] Jinbang, X., Anwen, S., Cheng, Y., Wenpei, R., Xuan, Y., "ANN based on IncCond algorithm for MPP tracke"r. *In: Bio-Inspired Computing: Theories and Applications (BIC-TA). 2011 Sixth International Conference*, pp. 129–134.

[51] Ramaprabha, R., Mathur, B.L., "Intelligent controller based maximum power point tracking for solar PV system. *Int. J. Comput. Appl*. (0975–8887) 12 (10).

[52] Messai, A., Mellit, A., Guessoum, A., Kalogirou, S.A., "Maximum power point tracking using GA optimize fuzzy logic controller and its FPGA implementation". *Sol. Energy* 86, 265–277.

[53] Subiyanto, Mohamed, A., Shareef, H., "Neural network optimized fuzzy logic controller for maximum power point tracking in a photovoltaic system". *Int. J. Photoenergy*, 6–13.

[54] Khaehintung, N., Pramotung, K., Tuvirat, B., Sirisuk, P., "RISC-microcontroller built-in fuzzy logic controller of maximum power point tracking for solarpowered light-flasher applications". *Indust Electron Soc, IECON 30th Annu Conf IEEE*, vol. 3, pp. 2673–2678.

[55] Alajmi, B.N., Ahmed, K.H., Finney, S.J., Williams, B.W., 2011. Fuzzy-logic-control approach of a modified hill-climbing method for maximum power point in microgrid standalone photovoltaic system. IEEE Trans. Power Electron. 26, 1022–1030.

[56] Kchaou A., Naamane A., Koubaa Y., M'sirdi N., "Second order sliding mode-based MPPT control for photovoltaic applications", *Sol. Energy* 155, 758–769.

[57] Li Shaowu, Liao Honghua, Yuan Hailing, Ai Qing, Chen Kunyi, "A MPPT strategy with variable weather parameters through analyzing the effect of the DC/DC converter to the MPP of PV system, *Sol. Energy* 144, 175–184.

[58] Mohamed Orabi, Ahmed Shawky, "Proposed Switching Losses Model for Integrated Point of Load Synchronous Buck Converters", IEEE Transactions on Power Electronics 2015; 30(9): 5136 - 5150